Available online at www.sciencedirect.com

ScienceDirect

Applied Catalysis B: Environmental 83 (2008) 123–130

APPLIED CATALYSIS B: ENVIRONMENTAL

www.elsevier.com/locate/apcatb

Promotion effect of tungsten oxide on photo-assisted selective catalytic reduction of NO with NH_3 over TiO_2

Seiji Yamazoe [a], Yasuyuki Masutani [a], Kentaro Teramura [b], Yutaka Hitomi [a], Tetsuya Shishido [a], Tsunehiro Tanaka [a,*]

[a] Department of Molecular Engineering, Graduate School of Engineering, Kyoto University, Kyoto 615-8510, Japan
[b] Kyoto University Pioneering Research Unit for Next Generation, Kyoto University, Kyoto 615-8510, Japan

Received 6 December 2007; received in revised form 17 January 2008; accepted 26 January 2008
Available online 9 February 2008

Abstract

The activity of TiO_2 in photo-assisted selective catalytic reduction of NO with NH_3 (photo-SCR) was tested by using a flow reactor. The activity of TiO_2 increased with increase in the amount of acid site. Density functional theory (DFT) calculations suggest that the rate of the NH_2NO decomposition, which is the rate-determining step of the photo-SCR, on the weak acid site is faster than that on the strong acid site. The activity of the photo-SCR was enhanced by the addition of a small amount of WO_3 on TiO_2 and 1.5 wt.% WO_3/TiO_2 showed the highest activity among the tested. According to the NH_3 adsorption experiments, the photo-SCR activity of WO_3/TiO_2 depends on the amount of the weak acid site. This result corresponds to the calculations by DFT. We concluded that the amount of the weak acid site on the catalyst is an important factor for the photo-SCR activity.

Keywords: TiO_2; Photocatalyst; SCR; NH_3; NO; WO_3; WO_3/TiO_2; DFT; Acid site; Acid strength

1. Introduction

It is important to remove NO_x contained in the exhaust gases at the stationary and mobile emission sources because NO_x is an air pollutant gas to be responsible for town smog and acid rain [1,2]. In the stationary emission sources, selective catalytic reduction technique with NH_3 (NH_3-SCR) in the presence of O_2 over V_2O_5–TiO_2-based catalysts is currently used in order to remove NO_x in the exhaust gas [1,3–5]. However, it is necessary to develop an NH_3-SCR system that can be operated at low temperature (<453 K) because the conventional catalysts require high temperature (573–673 K) to enough activity in the NH_3-SCR [6–11]. Up to now, many efforts have been directed to develop the low temperature NH_3-SCR system [7,11–13]. Singoredjo et al. [14] reported that MnO_2–Al_2O_3 showed high activity for the NH_3-SCR at 435 K. Recently, Qi and Yang [15] reported MnO_2–CeO_2 exhibits the good NH_3-SCR performance at 393 K.

In the previous study, we have reported that TiO_2 photocatalyst showed high catalytic activity for the photo-assisted selective catalytic reduction (photo-SCR) of NO with NH_3 (95% NO conversion and 96% N_2 selectivity at gas hourly space velocity (GHSV) = 8000 h^{-1}) even at room temperature [16,17]. However, the photo-SCR activity decreased with increasing GHSV. From the standpoint of practical use, it is necessary to enhance the photo-SCR activity at high GHSV (>16,000–20,000 h^{-1}).

We have reported that the reaction mechanism of the photo-SCR over TiO_2 [18–20], as shown in Scheme 1. NH_3 adsorbed on a Lewis acid site generates NH_2 radical by trapping a photo-formed hole. Then the NH_2 radical reacts with NO to form nitrosoamide (NH_2NO) species. The NH_2NO species is decomposed to N_2 and H_2O. Finally, Ti^{3+} site, formed from Ti^{4+} site by trapping an electron, is reoxidized by O_2. Additionally, kinetic study revealed that the rate-determining step of the photo-SCR over TiO_2 is the process of the decomposition of the NH_2NO species. Thus, the photo-SCR activity would be enhanced by the promotion of the NH_2NO decomposition rate. Darbeau et al. [21] reported that the decomposition rate of nitrosoamide derivatives depends on the

* Corresponding author. Tel.: +81 75 383 2558; fax: +81 75 383 2561.
E-mail address: tanakat@moleng.kyoto-u.ac.jp (T. Tanaka).

0926-3373/$ – see front matter © 2008 Elsevier B.V. All rights reserved.
doi:10.1016/j.apcatb.2008.01.032

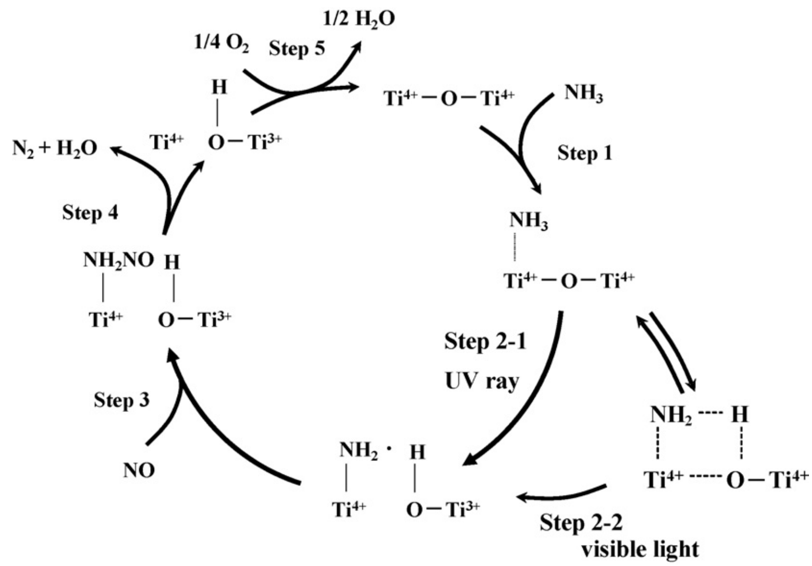

Scheme 1. Proposed reaction mechanism of the photo-SCR over TiO_2.

electronic state of themselves. Since NH_2NO species is formed on the acid site, it is expected that the NH_2NO decomposition rate is affected by the acid strength of catalyst.

It is known that the tungsten oxide on TiO_2 not only increases the amount of acid site but also changes the acid strength of TiO_2 [22–25]. In this study, we investigated the effect of loading amount of tungsten oxide on the photo-SCR activity and discussed the relationship between the photo-SCR activity and the acid property (acid strength and amount of acid site of catalysts). Additionally, we carried out density functional theory (DFT) calculations to elucidate the relationship between the NH_2NO decomposition rate and the acid strength.

2. Experimental

2.1. Preparation of catalysts

TiO_2 used in this study is Super Titania F-6 (Lot No. H04320) kindly supplied from SHOWA DENKO. This sample was hydrated in distilled water at 353 K for 2 h and filtered with suction, followed by drying at 383 K overnight. Dried sample was calcined in dry air at 673 K for 3 h. The specific surface area of prepared TiO_2 was $77\ m^2\ g^{-1}$ determined by N_2 adsorption. The crystal phase of prepared TiO_2 was determined by a SHIMADZU XD-D1 X-ray diffractometer using Cu Kα radiation. This sample consists of 91.3% anatase and 8.7% rutile. WO_3/TiO_2 catalysts were prepared by the impregnation method followed by evaporation to dryness. Super Titania F-6 were impregnated with aqueous solutions of ammonium tungstate *para*-pentahydrate and concentrated at 353 K. After these samples were dried at 383 K overnight, these were calcined in dry air at 673 K for 3 h. The specific surface area of prepared WO_3/TiO_2 sample was determined by N_2 adsorption. The specific surface areas of 1, 5 and 10 wt.% WO_3/TiO_2 were 77, 90 and 90 $m^2\ g^{-1}$, respectively.

2.2. Catalytic reaction

Photo-SCR reactions were carried out in a conventional fixed bed flow system at room temperature. Catalysts were fixed with quartz wool and filled a quartz reactor which had flat facet (50 mm × 10 mm × 1 mm). Before the reactions, catalysts were pretreated at 673 K by flowing 10% O_2 diluted with Ar at 50 ml min^{-1}. The typical reaction gas composition was as follows: NH_3, 1000 ppm; NO, 1000 ppm; O_2, 2%; Ar, balance. PerkinElmer PE300BF 300 W Xe lamp was used as a light source and samples were irradiated from the one side of the flat facets of the reactor with this lamp. N_2 and N_2O products were analyzed by a SHIMADSU GC-8A TCD gas chromatograph with MS-5A column for N_2 detection and Chromosorb 103 for N_2O.

2.3. Fourier transform infrared (FT-IR) spectroscopy

The TiO_2 sample (100 mg) was cast into a self-supported disk (diameter = 12 mm). The molded sample was introduced into an in situ IR cell equipped with KBr windows. The sample was heated in air and evacuated for 30 min at 673 K, followed by treatment with 12.0 kPa O_2 for 60 min and evacuation for 30 min at 673 K before records of FT-IR spectra. Pyridine-adsorbed spectra were recorded with a Perkin–Elmer SPECTRUM ONE Fourier transform infrared spectrometer. The resolution of spectra was 4 cm^{-1} and the quantity survey number of time was 16.

2.4. Temperature-programmed desorption (TPD) of NH_3

NH_3-TPD was carried out to investigate the acid property of the catalysts. The experiments were performed on a TPD-1-ATW apparatus (Bel Japan Inc.) using 100 mg of catalyst. Prior to the experiments, the catalysts were pretreated at 673 K for 1 h in a pure He (50 ml min^{-1}) stream. The furnace temperature

was lowered to 373 K and the samples were then treated with NH_3 (1000 ppm in He) at a flow rate of 50 ml min^{-1} for 4 h. Physisorbed NH_3 was removed by flushing the catalyst with He (50 ml min^{-1}) at 373 K for 0.5 h before starting the TPD experiments. Experimental runs were recorded by heating the sample in He (50 ml min^{-1}) from 373 to 823 K at a heating rate of 5 K min^{-1} and finally keeping the temperature constant for 1 h at 823 K to ensure complete ammonia desorption.

2.5. DFT calculation method

Quantum chemical calculations using DFT were carried out in order to estimate the relationship between the decomposition rate of NH_2NO species and the acid strength of Lewis acid site. The decomposition reaction of NH_2NO species is independent on photo-excitation process, as shown in Scheme 1. Therefore, the photo-excitation of TiO_2 is ignored in this study. Onal et al. [26] reported that the adsorption of small molecules such as H_2O and NH_3 is a relatively local phenomenon and a small metal oxide cluster can sufficiently represent larger cluster surfaces. Therefore, the neutral $Ti^{4+}O_5H_6$ cluster model representing anatase phase was used, as a model of Lewis acid site. We created a series of TiO_5H_6 models having different Lewis acid strength by moving the position of Ti site. DFT calculations were conducted using Becke's three parameter hybrid (B3LYP) method involving Lee et al. correlation function [27,28] for TiO_5H_6, NH_3-adsorbed TiO_5H_6 and NH_2NO–TiO_5H_6 cluster models, according to the report of Onal et al. [26]. The basis set used in the DFT calculations was 6-31G provided in Gaussian '03. The neutral cluster model of TiO_5H_6 is obtained from the structure of anatase TiO_2 (space group: $I4_1/amd$; lattice parameter: a, b = 3.785 Å, c = 9.514 Å) by saturating the peripheral oxygen atoms with hydrogen atoms. The acid strength of the calculated TiO_5H_6 cluster models were estimated from the adsorption energy of NH_3. The decomposition rate of NH_2NO species was estimated from the decomposition energy of NH_2NO species using linear free energy relation (LFER).

3. Results and discussion

3.1. DFT calculations

In our previous study, we have proposed the reaction mechanism of the photo-SCR (Eley–Rideal mechanism as shown in Scheme 1) and the photo-SCR proceeds over acid site on TiO_2 [17,18]. Additionally, we have determined that the rate-determining step is the decomposition of NH_2NO species [19]. Therefore, the increase in the acid amount and/or the decomposition rate of NH_2NO species would enhance the photo-SCR activity. It is known that the decomposition rate of NH_2NO species depends on the electronic density of N atom of NH_2 in NH_2NO derivatives [21]. In the photo-SCR, NH_2NO species is formed on Lewis acid site of TiO_2. Therefore, the acid strength of Lewis acid site would be an important factor for the photo-SCR activity because the electronic density of N atom of NH_2 in NH_2NO derivatives should depend on the acid strength. In this study, we carried out the DFT calculation to investigate the relationship between the acid strength and the decomposition rate of NH_2NO.

Onal et al. [26] reported that the adsorption of small molecules such as NH_3 is a relatively local phenomenon and a small metal oxide cluster can sufficiently represent larger cluster surfaces. As a model of Lewis acid site, mononuclear TiO_5H_6 with all of the peripheral oxygen atoms saturated by hydrogen atoms was used in this study. Fig. 1a shows the TiO_5H_6 model representing anatase structure of TiO_2. The positions of oxygen and hydrogen atoms were fixed and the position of Ti atom was moved up and down along Z-axis to change the coordination environment. Fig. 1b–d shows the models that Ti atom of Fig. 1a is moved −0.1, 0.1 and 0.15 Å on Z-axis, respectively, and the distance of Ti–O1 of each model is

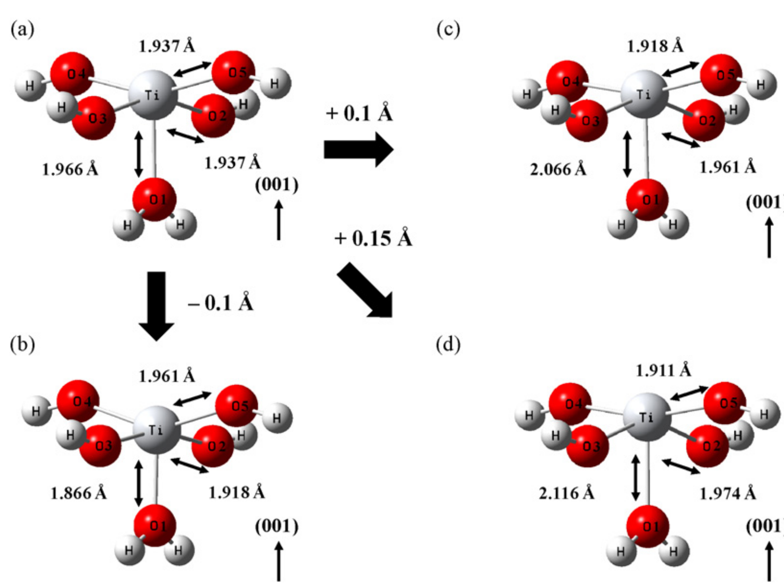

Fig. 1. TiO_5H_6 models used in the DFT calculation: TiO_5H_6 model (a) representing anatase TiO_2 structure, (b) that Ti atom of model (a) are moved −0.1 Å on Z-axis, (c) that Ti atom of model (a) are moved 0.1 Å on Z-axis, and (d) that Ti atom of model (a) are moved 0.15 Å on Z-axis.

Table 1
NH_3 adsorption and NH_2NO decomposition energies of TiO_5H_6 models

TiO_5H_6 model	Distance of Ti–O1 (Å)	E_{NH_3ad} [a] (kcal mol^{-1})	E_{dec} [b] (kcal mol^{-1})
Fig. 1a	1.966	−28.26	−37.98
Fig. 1b	1.866	−24.39	−38.53
Fig. 1c	2.066	−31.96	−37.01
Fig. 1d	2.116	−33.75	−36.41

[a] Adsorption energy of NH_3.
[b] Decomposition energy of NH_2NO.

Table 2
Mulliken atomic charges of Ti and O atoms in TiO_5H_6 models

Atom	Fig. 1a	Fig. 1b	Fig. 1c	Fig. 1d
Ti	1.432	1.426	1.428	1.423
O1	−0.7172	−0.7213	−0.7100	−0.7060
O2	−0.8049	−0.8034	−0.8043	−0.8031
O3	−0.8049	−0.8034	−0.8043	−0.8031
O4	−0.7672	−0.7744	−0.7577	−0.7525
O5	−0.7672	−0.7744	−0.7577	−0.7525

listed in Table 1. Additionally, electronic states of all models are calculated and obtained Mulliken atomic charges of Ti and O atoms are listed in Table 2. The order of the Mulliken atomic charge of Ti atom is in Fig. 1a > c > b > d.

Fig. 2 shows NH_3-adsorbed TiO_5H_6 models whose NH_3 was geometrically optimized by DFT calculations. The Ti–N distance (2.249 Å) of the model in Fig. 1b was longest in all the models and the Ti–N distance shortened with moving Ti atom upon Z-axis. The acid strength of each model was estimated by the adsorption energy (E_{NH_3ad}) of NH_3. E_{NH_3ad} was defined as

$$E_{NH_3ad} = E_{NH_3-cluster} - (E_{cluster} + E_{NH_3})$$

where $E_{NH_3ad-cluster}$, $E_{cluster}$ and E_{NH_3} are the calculated energies of NH_3-adsorbed TiO_5H_6 model, TiO_5H_6 model and NH_3, respectively. Calculated E_{NH_3ad} values were listed in Table 1. The model in Fig. 1b had the lowest $|E_{NH_3ad}|$ energy (24.39 kcal mol^{-1}) and the value of E_{NH_3ad} increased as the Ti–N distance decreased. The larger $|E_{NH_3ad}|$ is, the stronger Lewis acid strength is. The order of the acid site strength of the models is in Fig. 1d > c > a > b. This order is different from that of the atomic charge of Ti atom, indicating that the acid strength is hard to explain on the basis of the atomic charge of Ti atom.

The decomposition energy (E_{dec}) of NH_2NO species was calculated for each model. Fig. 3 shows NH_2NO-adsorbed TiO_5H_6 models whose NH_2NO was geometrically optimized by DFT calculations. The value of E_{dec} was defined as

$$E_{dec} = (E_{cluster} + E_{N_2} + E_{H_2O}) - E_{NH_2NO-cluster}$$

where E_{N_2}, E_{H_2O} and $E_{NH_2NO-cluster}$ are the calculated energies of N_2, H_2O and NH_2NO-adsorbed TiO_5H_6 model, respectively. The calculated results were listed in Table 1. Fig. 1b model showed the largest $|E_{dec}|$ (38.53 kcal mol^{-1}) in all the models. The $|E_{dec}|$ value decreased with increasing the acid strength. Some researchers proposed that NH_2NO species is decomposed to N_2 and H_2O via some intermediates involving NHNOH [29–31]. However, it has not been clarified the exact decomposition mechanism of NH_2NO species. On the basis of LFER, it can be estimated that the order of the activation energy of NH_2NO decomposition for each model in Fig. 1 would be Fig. 1d > c > a > b. Therefore, the model in Fig. 1b shows

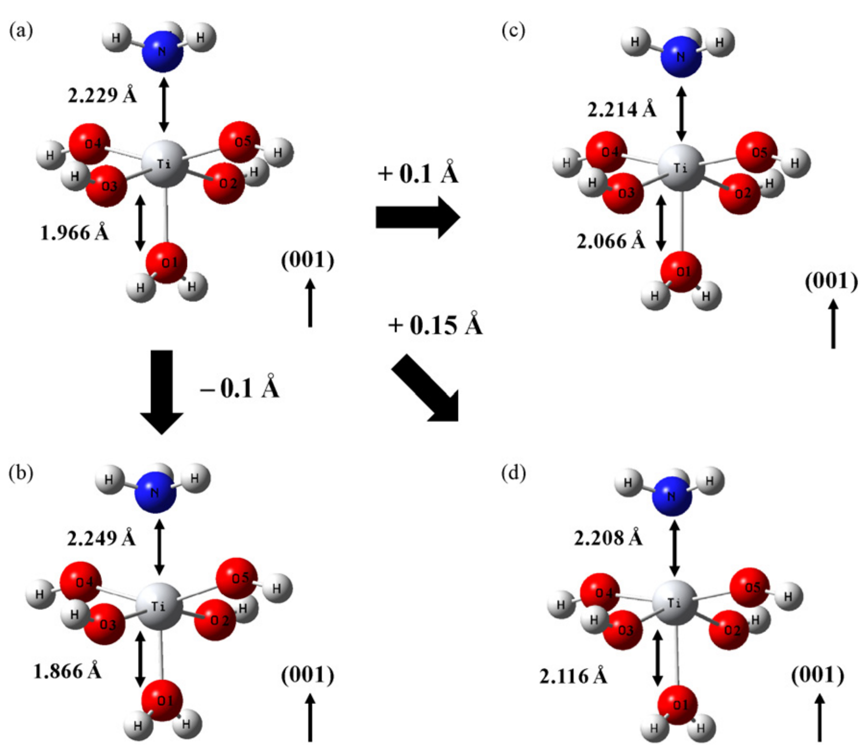

Fig. 2. The structures of the optimized NH_3-adsorbed model of (a) Fig. 1a, (b) Fig. 1b, (c) Fig. 1c, and (d) Fig. 1d.

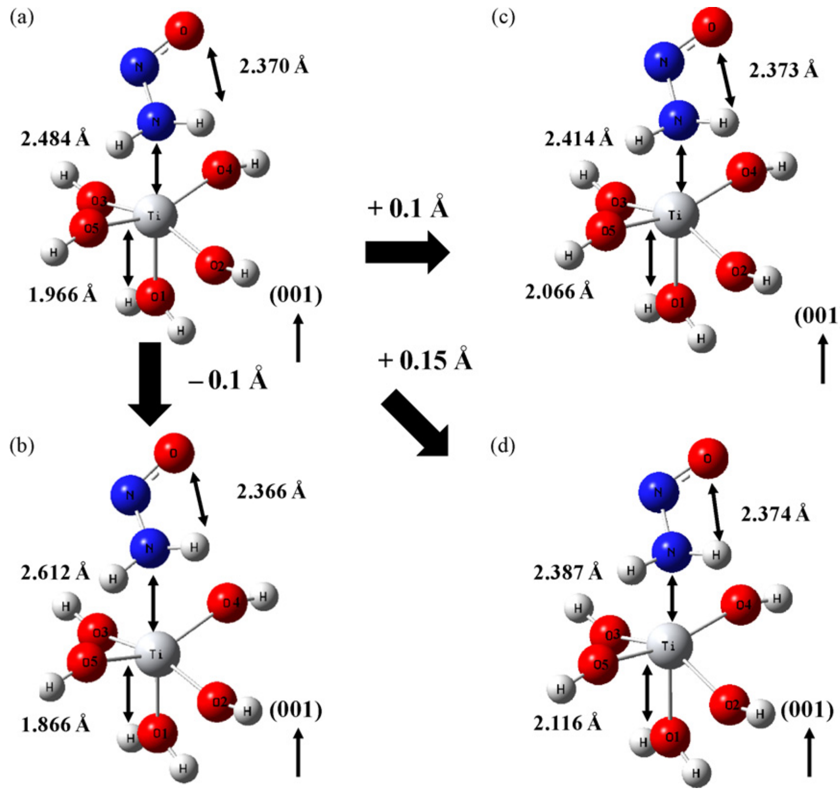

Fig. 3. The structures of the optimized NH_2NO-adsorbed model of (a) Fig. 1a, (b) Fig. 1b, (c) Fig. 1c, and (d) Fig. 1d.

the largest NH_2NO decomposition rate. This order was in accordance with the strength of Lewis acid site. Thus, we conclude that the weak acid site has larger NH_2NO decomposition rate than the strong acid site.

3.2. Photo-SCR reaction over WO_3/TiO_2 catalysts

In the previous section, DFT calculations show that the weak acid site shows higher NH_2NO decomposition rate than that on strong acid site. Thus, the increase in the amount of weak acid site would lead to high photo-SCR activity. It is known that not only the amount of acid site but also the acid strength on TiO_2 are changed by the addition of tungsten oxide [22–25]. The effect of loading amount of tungsten oxide over TiO_2 on the photo-SCR activity was investigated. Activities of WO_3/TiO_2 catalysts for the photo-SCR at GHSV = 32,000 h^{-1} are shown in Table 3. Bare TiO_2 showed 63% NO conversion. The increase in the content of WO_3 enhanced the photo-SCR activity and 1.5 wt.% WO_3/TiO_2 exhibited the highest activity (NO conversion: 77%). Moreover, 1.5 wt.% WO_3/TiO_2 showed

Table 3
The photo-SCR activity and the acidity of the samples

Catalyst	NO conv.[a] (%)	N_2 selec.[b] (%)	$N_{total\ acid\ site}$[c] (μmol g^{-1})	$N_{weak\ acid\ site}$[d] (μmol g^{-1})	$N_{strong\ acid\ site}$[e] (μmol g^{-1})
TiO_2	63[f]	>99	420	120	300
0.5WT[g]	68[f]	>99	430	120	310
1WT[g]	74[f]	>99	430	130	300
1.5WT[g]	77[f]	>99	460	165	295
	96[h]	>99			
2WT[g]	74[f]	>99	460	160	300
3WT[g]	59[f]	>99	440	120	320
5WT[g]	52[f]	>99	440	110	330
10WT[g]	52[f]	>99	450	140	310
15WT[g]	37[f]	>99	460	30	430

[a] NO conversion.
[b] N_2 selectivity.
[c] Total amount of the acid site.
[d] Amount of the weak acid site, which desorbs NH_3 under 373 K.
[e] Amount of the strong acid site, which desorbs NH_3 above 373 K.
[f] Photo-SCR activity at GHSV = 32,000 h^{-1}.
[g] *x*WT means *x* wt.% WO_3/TiO_2.
[h] Photo-SCR activity at GHSV = 25,000 h^{-1}.

high and stable activity at GHSV = 25,000 h^{-1}. The highest activity (96% NO conversion and 99% N_2 selectivity (by-product: N_2O)) indicating that 1.5 wt.% WO_3/TiO_2 is the efficient catalyst for the photo-SCR.

3.3. Acid property of WO_3/TiO_2 catalysts

Fig. 4a shows the FT-IR spectrum of pyridine adsorbed on TiO_2. Bare TiO_2 exhibited four bands at 1445, 1493, 1576 and 1604 cm^{-1}. These bands are attributed to pyridine coordinated to Lewis acid sites [32]. The band due to adsorbed pyridinium ion on Brönsted acid sites (1520–1550 cm^{-1}) [33,34] was not recorded. This result is accordance with previous report [5,7,32,35]. The FT-IR spectra of pyridine adsorbed on 1 and 10 wt.% WO_3/TiO_2 are shown in Fig. 4b and c. Only the bands due to the coordinated pyridine to Lewis acid sites were detected and the formation of Brönsted acid sites was not obtained. These results indicate that the type of the acid site does not change by the addition of WO_3 on TiO_2.

The total amounts of the acid site of all the samples were determined by the amount of NH_3 chemisorption. The acid amount for each sample was listed in Table 3. Bare TiO_2 showed the acid amount of 420 μmol g^{-1}. The acid amount was slightly increased by the addition of WO_3 and 1.5 wt.% WO_3/TiO_2 exhibited 460 μmol g^{-1}. The rate-determining step of the photo-SCR is the decomposition of NH_2NO

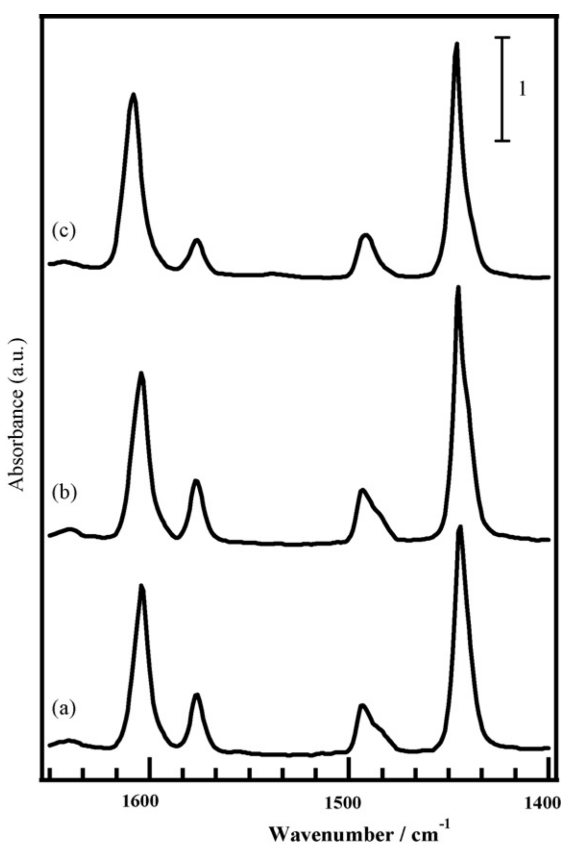

Fig. 4. FT-IR spectra of pyridine adsorbed (a) bare TiO_2, (b) 1 wt.% WO_3/TiO_2, and (c) 10 wt.% WO_3/TiO_2.

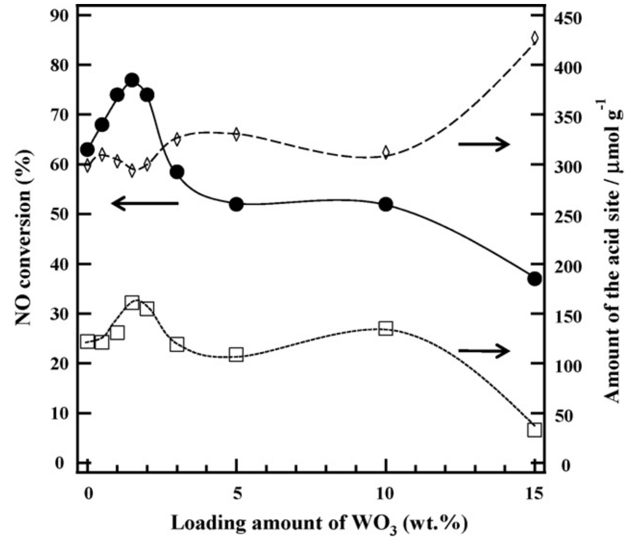

Fig. 5. The photo-SCR activity (●), the amount of the weak acid site (□) and the amount of the strong acid site (◇) as a function of the loading amount of WO_3.

species and NH_2NO species is generated on Lewis acid site on TiO_2, suggesting that the photo-SCR activity depends on the acid amount. However, the photo-SCR activity did not show clear relationship with the loading amount of WO_3. Next, we investigated the effect of the acid strength on the photo-SCR activity. Fig. 5 shows both the photo-SCR activity and the amount of acid site as a function of the loading amount of WO_3. We defined the acid site that desorbs chemisorbed NH_3 at <373 K as weak acid and the acid site that desorbs chemisorbed NH_3 above 373 K as strong acid. 1.5 wt.% WO_3/TiO_2 has the largest amount of weak acid sites among the tested catalysts. Moreover, the amount of the weak acid site shows good correlated with the photo-SCR activity. On the other hand, the amount of strong acid site hardly changed up to 10 wt.% WO_3/TiO_2 and then increased with the loading amount of WO_3. This behavior of the amount of the strong acid site as a function of the addition of WO_3 disagreed with that of the photo-SCR activity. These results clearly indicate that the photo-SCR depends on the weak acidity of the catalyst. This result accords with the results of the DFT calculations. The DFT calculations indicate that the weak acid site promotes the decomposition rate of the NH_2NO species, which is the rate-determining step of the photo-SCR reaction. The enhancement of the decomposition rate of the NH_2NO species by the increase in the amount of the weak acid site would lead to the high activity at 1.5 wt.% WO_3/TiO_2 sample. Fig. 6 shows the NH_3-TPD profiles of the samples. Bare TiO_2 and 0.5–2 wt.% WO_3/TiO_2 samples showed the similar TPD profiles. Further addition of WO_3 (5 and 10 wt.% samples) made the NH_3-desoption temperature high. The formation of the stronger acid site would cause the agglomeration of WO_3 species loaded on TiO_2. From the above results, we conclude that the photo-SCR activity depends on the acid strength of the catalyst and that the amount of the weak acid site is the key factor for the photo-SCR.

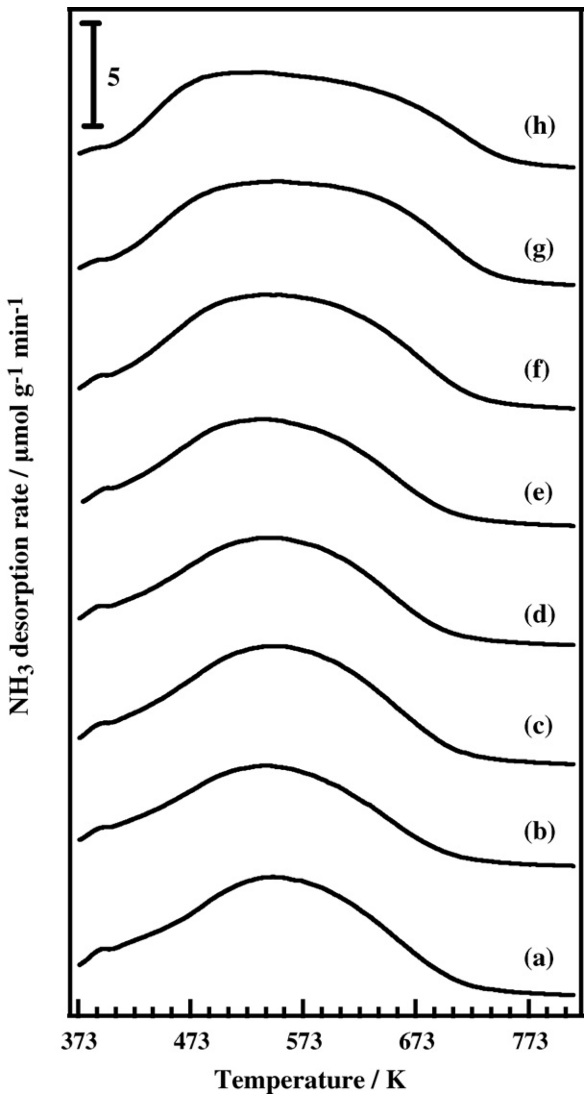

Fig. 6. NH_3-TPD profiles of (a) bare TiO_2, (b) 0.5 wt.% WO_3/TiO_2, (c) 1 wt.% WO_3/TiO_2, (d) 1.5 wt.% WO_3/TiO_2, (e) 2 wt.% WO_3/TiO_2, (f) 5 wt.% WO_3/TiO_2, (g) 10 wt.% WO_3/TiO_2, and (h) 15 wt.% WO_3/TiO_2.

4. Conclusion

DFT calculations were employed to investigate the relationship between the acid strength and evaluated decomposition rate of the NH_2NO derivatives on the Ti site with various Lewis acid strength, because the NH_2NO decomposition is the rate-determining step of the photo-SCR. The calculation results indicate that the decomposition rate of the NH_2NO species is enhanced as the acid strength becomes weak. We carried out the photo-SCR over TiO_2 catalysts modified by the addition of WO_3 to increase the photo-SCR activity. The photo-SCR activity increased upon the addition of WO_3 up to 1.5 wt% WO_3 and 1.5 wt.% WO_3/TiO_2 catalyst showed the highest activity. Further addition of WO_3, the photo-SCR activity decreased. The photo-SCR performance was not correlated to the type and the total amount of the acid site. The amount of the weak acid site was well correlated with the photo-SCR activity. 1.5 wt.% WO_3/TiO_2 showed the best performance and has the largest amount of the weak acid site among tested catalysts. This correlation accords with the DFT calculation results. Therefore, we concluded that the weak acid site is the important factor for the photo-SCR activity.

Acknowledgements

S. Yamazoe is supported by a JSPS Research Fellowship for Young Scientists. The authors thank Prof. Masashi Inoue, Dr. Shinji Iwamoto and Dr. Saburo Hosokawa for the measurement of NH_3-TPD.

References

[1] V. Parvulescu, P. Grange, B. Delmon, Catal. Today 46 (1998) 233.
[2] S. Wood, Chem. Eng. Prog. 90 (1994) 32.
[3] H. Bosch, F. Janssen, Catal Today 2 (1988) 369.
[4] S. Cho, Chem. Eng. Prog. 90 (1994) 39.
[5] G. Busca, L. Lietti, G. Ramis, F. Berti, Appl. Catal. B 18 (1998) 1.
[6] W. Kijlstra, D. Brands, H. Smit, E. Poels, A. Bliek, J. Catal. 171 (1997) 219.
[7] D. Pena, B. Uphade, P. Smirniotis, J. Catal. 221 (2004) 421.
[8] G. Centi, S. Perathoner, D. Biglino, E. Giamello, J. Catal. 151 (1995) 75.
[9] G. Ramis, L. Yi, G. Busca, M. Turco, E. Kotur, R.J. Willey, J. Catal. 157 (1995) 523Y.
[10] A. Kato, S. Matsuda, F. Nakajima, M. Imanri, I. Watanabe, J. Phys. Chem. 85 (1981) 1710.
[11] R. Long, R. Yang, R. Chang, Chem. Commun. (2002) 452.
[12] E. Garcia-Bordeje, J. Pinilla, M. Lazaro, R. Moliner, J. Fierro, J. Catal. 233 (2005) 166.
[13] M. Richter, A. Trunschke, U. Bentrup, K. Brzezinka, E. Schreier, M. Schneider, M. Pohl, R. Fricke, J. Catal. 206 (2002) 98.
[14] L. Singoredjo, R. Korver, F. Kapteijn, J. Moulijn, Appl. Catal. A 1 (1992) 297.
[15] G. Qi, R. Yang, Chem. Commun. (2003) 848.
[16] S. Yamazoe, T. Okumura, K. Teramura, T. Tanaka, Catal. Today 111 (2006) 266.
[17] T. Tanaka, K. Teramura, K. Arakaki, T. Funabiki, Chem. Commun. (2002) 2742.
[18] K. Teramura, T. Tanaka, T. Funabiki, Langmuir 19 (2003) 1209.
[19] K. Teramura, T. Tanaka, S. Yamazoe, K. Arakaki, T. Funabiki, Appl. Catal. B 53 (2004) 29.
[20] S. Yamazoe, K. Teramura, Y. Hitomi, T. Shishido, T. Tanaka, J. Phys. Chem. C 111 (2007) 14189.
[21] R.W. Darbeau, R.S. Pease, R.E. Gibble, J. Org. Chem. 66 (2001) 5027.
[22] T. Yamaguchi, Y. Tanaka, K. Tanabe, J. Catal. 65 (1980) 442.
[23] G. Ramis, G. Busca, C. Cristiani, L. Lietti, P. Forzatti, F. Bregani, Langmuir 8 (1992) 1744.
[24] Z. Ma, W.M. Hua, Y. Tang, Z. Gao, J. Mol. Catal. A 159 (2000) 335.
[25] J. Papp, S. Soled, K. Dwight, A. Wold, Chem. Mater. 6 (1994) 496.
[26] I. Onal, S. Soyer, S. Senkan, Surf. Sci. 600 (2006) 2457.
[27] M.J. Frisch, G.W. Trucks, H.B. Schlegel, G.E. Scuseria, M.A. Robb, J.R. Cheeseman, J.A. Montgomery Jr., T. Vreven, K.N. Kudin, J.C. Burant, J.M. Millam, S.S. Iyengar, J. Tomasi, V. Barone, C. Mennucci, M. Cossi, G. Scalmani, N. Rega, G.A. Pettersson, H. Nakatsuji, M. Hada, M. Ehara, K. Toyota, R. Fukuda, J. Hasegawa, M. Ishida, T. Nakajima, Y. Honda, O. Kitao, H. Nakai, M. Klene, X. Li, J.E. Knox, H.P. Hratchian, J.B. Cross, V. Bakken, C. Adamo, J. Jaramillo, R. Gomperts, R.E. Stratmann, O. Yazyev, A.J. Austin, R. Cammi, C. Pomelli, J.W. Ochterski, Y. Ayala, K. Morokuma, G.A. Voth, P. Salvador, J.J. Dannenberg, G. Zakrzewski, S. Dapprich, A.D. Daniels, M.C. Strain, O. Farkas, D.K. Malick, A.D. Rabuck, K. Raghavachari, J.B. Foresman, J.V. Ortiz, Q. Cui, A.G. Baboul, S. Clifford, J. Cioslowski, B.B. Stefanov, G. Lui, A. Liashenko, P. Piskorz, I. Komaromi, R.L. Martin, D.J. Fox, T. Keith, M.A. Al-Laham, C.Y. Peng, A.

Nanayakkara, M. Challacombe, P.M.W. Gill, B. Johnson, W. Chen, M.W. Wong, C. Gonzalez, J.A. Pople, Gaussian Inc., Wallingford, CT, 2004.
[28] C.T. Lee, W.T. Yang, R.G. Parr, Phys. Rev. B 37 (1988) 785.
[29] F. Gilardoni, J. Weber, A. Baiker, J. Phys. Chem. A 101 (1997) 6069.
[30] M. Anstrom, N.Y. Topsoe, J.A. Dumesic, J. Catal. 213 (2003) 115.
[31] X.L. Yin, H.M. Han, A. Miyamoto, Phys. Chem. Chem. Phys. 2 (2000) 4243.
[32] G. Busca, G. Ramis, Appl. Surf. Sci. 27 (1986) 114.
[33] C. Martin, I. Martin, C. Delmoral, V. Rives, J. Catal. 146 (1994) 415.
[34] E.P. Parry, J. Catal. 2 (1963) 371.
[35] J.M.G. Amores, V.S. Escribano, G. Ramis, G. Busca, Appl. Catal. B 13 (1997) 45.